Journal Pre-proof

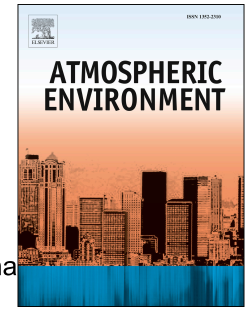

Investigating the relationship between aerosol and cloud optical properties inferred from the MODIS sensor in recent decades over East China

Jing Huang, Lingbing Bu, Kanike Raghavendra Kumar, Rehana Khan, N.S.M.P. Latha Devi

PII: S1352-2310(20)30546-X

DOI: https://doi.org/10.1016/j.atmosenv.2020.117812

Reference: AEA 117812

To appear in: *Atmospheric Environment*

Received Date: 28 April 2020

Revised Date: 21 July 2020

Accepted Date: 22 July 2020

Please cite this article as: Huang, J., Bu, L., Kumar, K.R., Khan, R., Devi, N.S.M.P.L., Investigating the relationship between aerosol and cloud optical properties inferred from the MODIS sensor in recent decades over East China, *Atmospheric Environment* (2020), doi: https://doi.org/10.1016/j.atmosenv.2020.117812.

CRediT author statement

All authors have read and agreed to the published version of the manuscript.

Jing Huang: Conceptualization, Formal analysis, Investigation, Visualization, Writing-original draft preparation. **Lingbing Bu:** Supervision, Funding Acquisition, Project Administration, Writing-review and editing. **Kanike Raghavendra Kumar:** Conceptualization, Investigation, Resources, Writing-review and editing. **Rehana Khan:** Data curation, Writing-review and editing. **N.S.M.P. Latha Devi:** Data curation and Language editing.

Graphical Abstract

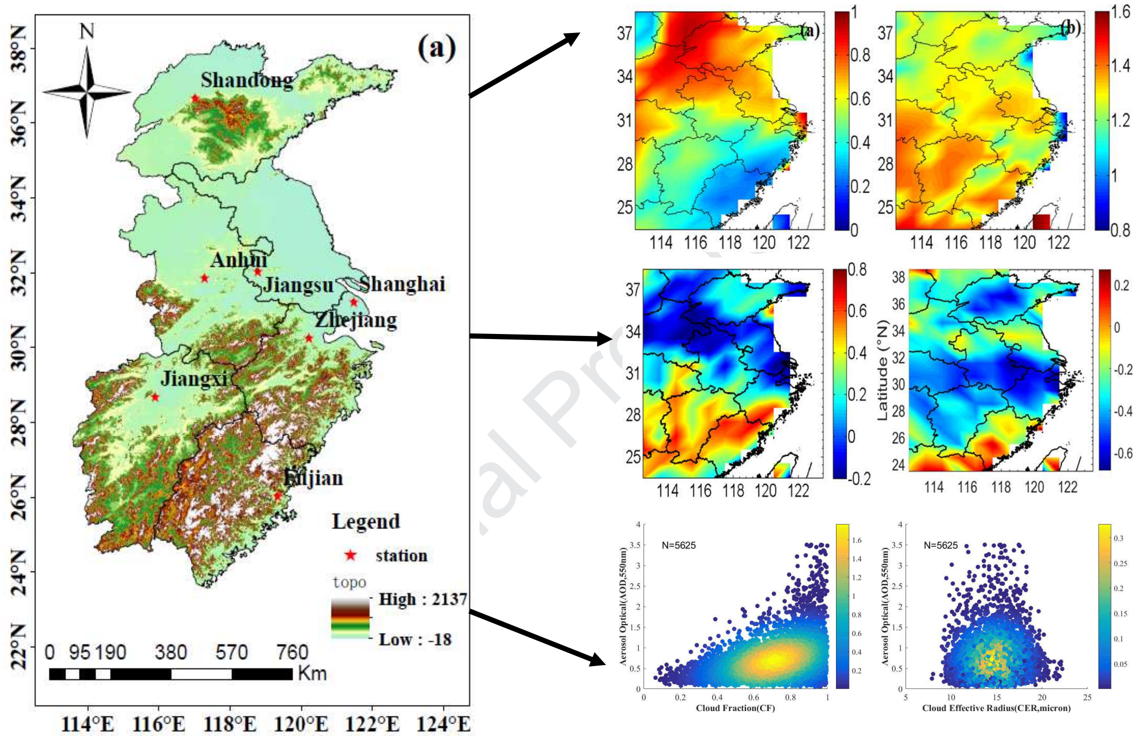

Investigating the relationship between aerosol and cloud optical properties inferred from the MODIS sensor in recent decades over East China

Jing Huang[a,c], Lingbing Bu[a,*], Kanike Raghavendra Kumar[b,a,**], Rehana Khan[a,d],

N.S.M.P. Latha Devi[b]

[a]Collaborative Innovation Centre for Forecast and Evaluation of Meteorological Disasters, Key Laboratory of Meteorological Disaster, Ministry of Education (KLME), International Joint Laboratory on Climate and Environment Change (ILCEC), Key Laboratory for Aerosol-Cloud-Precipitation of China Meteorological Administration, School of Atmospheric Physics, Nanjing University of Information Science and Technology, Nanjing 210044, Jiangsu, China.

[b]Department of Physics, Koneru Lakshmaiah Education Foundation (KLEF), Vaddeswaram 522502, Guntur, Andhra Pradesh, India.

[c]Anhui Meteorological Observation Technical Center, Hefei, Anhui, China.

[4]Department of Physics, Higher Education, Government of Khyber Pakhtunkhwa, Peshawar, 25000, Pakistan.

*****Corresponding author(s):
lingbingbu@nuist.edu.cn (L. Bu);
kanike.kumar@gmail.com, rkkanike@kluniversity.in (K. R. Kumar)

Abstract

In the present paper, we have analyzed the spatiotemporal distributions and trends of aerosol optical depth observed at 550 nm (AOD_{550}), and its relation with the optical properties of clouds over East China. For this purpose, we have used the long-term (2000-2017) data obtained from the Moderate-resolution Imaging Spectroradiometer (MODIS) Terra satellite to examine and understand the existing relationship between them. The spatial gradient of AOD_{550} showed an increase from the South to the North of the study domain. However, the seasonal variation of AOD_{550} was found high in summer and low during the winter. We have noticed a significant increasing trend in AOD over the northern part of the study area, especially in autumn and winter seasons. The study also investigated the spatial and temporal changes to understand the relationship between AOD and cloud properties, namely cloud fraction (CF), cloud top temperature (CTT), Cloud effective radius (CER) and cloud top pressure (CTP), respectively. Besides, the linear regression analysis was conducted to estimate the time series trend for the aerosol and cloud properties during the study period. Further, the regional correlation maps were adopted to improve our understanding of the existing relationship between aerosol and cloud properties. A positive correlation between AOD and CF and CER is evident in most of the places in East China.

Keywords: MODIS; Aerosol optical depth; Cloud optical depth; Cloud fraction; Cloud effective radius; East China.

1. Introduction

Atmospheric aerosols have a significant effect on clouds and earth radiation budget. The role of atmospheric aerosols in causing climate change, mainly on regional scales, cannot be ignored. They have visible effects on human health, climate, and air quality; and indirectly influence physical properties and lifetime of clouds by serving as cloud condensation nuclei (CCN) (Qin et al., 2018). The long-term spatiotemporal variability in aerosol optical depth (AOD) works as an essential input for the studies related to clouds formation, climate change, and Earth's radiation budget. Aerosols have been previously recounted to be as the source of uncertainty that significantly affects the earth's weather and climatic radiative system in many ways. They alter both 'direct' through their ability to scatter and absorb solar radiation and 'indirect' by modifying the microphysics of clouds (IPCC, 2013).

Consequently, the long-term regional scale and high temporal resolved measurements are required to understand and quantify the microphysical impact of both natural and anthropogenic aerosols on cloud properties and to improve the uncertainties associated with these impacts. Most research publications to date have shown that aerosols play an essential role in the formation and life cycle of clouds by changing the size and density of cloud droplets. Increasing aerosols cause an increase in CCN concentrations, leading to denser cloud drop concentrations and a decrease in the droplet size under constant liquid water content. It is known as the "first indirect effect" or "Twomey effect" (Twomey, 1977).

Since smaller cloud droplets affect the efficiency of rain, causing an increase in liquid water content, cloud lifetime and cloud cover known as the "second indirect effect" or "cloud lifetime effect" (Twomey, 1977). Further, tropospheric aerosols are also very prevalent types especially, with regional new particle formation sub-micron range (secondary aerosols), which are produced through the gas-to-particle conversion processes. This phenomenon leads to a lower rate of surface evaporation and increasing atmospheric stability (Myhre et al., 2007). Aerosol indirect effects lie on the aerosol type, their vertical and size distribution, and meteorological conditions (Yuan et al., 2008). Both the first and second indirect effects relieve the pressure of global warming by cooling the atmosphere (Myhre et al., 2007). However, the presence of soot particles (absorbing aerosols) such emitted from the biomass burning may prevent cloud formation by reducing the moisture available in the troposphere for cloud growth, known as a semi-direct effect (Ackerman et al., 2000).

Notwithstanding the significance of the climatic effect of aerosols and the importance of clouds, many investigations were conducted over China since the launch of Moderate-resolution Imaging Spectroradiometer (MODIS) sensor with the onboard Terra and Aqua satellites (Luo et al., 2014; Kumar et al., 2014, 2018; Kumar, 2014; Adesina et al., 2016; Kang et al., 2015, 2016; He et al., 2012, 2016; Hu et al., 2018; Boiyo et al., 2018). More recently, satellite analyses have revealed a persistent relation between aerosol and cloud optical properties (Kumar et al., 2018; Kumar, 2014; Adesina et al., 2016; Kang et al., 2015; Sharif et al., 2015). As far as, we know only a few studies had highlighted the existing relationship between AOD and different cloud properties over the mainland of China, but not much has been done over the present region of interest, particularly East China (Yuan et al., 2008; Kang et al., 2015; Tang et al., 2014). Kang et al. (2015) reported their relationship through correlation studies over entire China, particularly in the provincial capitals using the

MODIS data from 2000 to 2013. Tang et al. (2014) examined the aerosol-cloud properties relation over the north china region, provided limited analysis with a short span of the data period. However, none of the authors have much concentrated and investigated understanding their relationships and further assessment of regional climate change over East China. To the best of our knowledge, the present work dealt with studying the aerosol and cloud properties relation and firmly believes it provides an opportunity to fill the knowledge gap in the country. The primary objectives of the study are as follows. The first objective is to investigate the spatiotemporal variations of aerosol optical properties such as AOD, Ångström exponent (AE), and water vapor (WV) over East China based on the 18-years (2000–2017) of data derived from the MODIS onboard Terra satellite. Whereas, the second objective is to understand the relation of aerosols with the cloud microphysical properties such as cloud fraction (CF), cloud effective radius (CER), cloud top pressure (CTP), and cloud top temperature (CTT).

2. Data and Methods

2.1. Study domain

The selected study domain is East China, situated approximately between 24–38°N and 113–123°E, shown with the location of selected regions on the topography map (Fig. 1a). The present study has been carried out over East China domain consist of 8 significant capitals cities, namely Shandong (Provincial capital is Jinan, JN), Jiangsu (Nanjing, NJ), Anhui (Hefei, HF), Zhejiang (Hangzhou, HZ), Jiangxi (Nanchang, NC), Fujian (Fuzhou, FZ; Xiamen, XM), and Shanghai (Shanghai City, SH). The study domain is with rapid economic development as the most urbanized and industrialized regions are located in this part of China. This region as a whole has the highest AOD with a typical value of 0.6, resulted from the densely populated and nation's largest agriculture zone releases a considerable quantity of aerosols (Kang et al., 2016, 2020; He et al., 2012, 2016; Hu et al., 2018). Moreover, the study region has a low elevation above the mean sea level (Table 1), with the Huaihe River Basin as the demarcation line.

The study area is located in the eastern Asian monsoon zone with four distinctive seasons: spring (March-May), summer (June-August), autumn/fall (September-November), and winter (December-February). The southern portion of East China is a subtropical monsoon climate region, and the North area is a temperate monsoon climate region. Due to the prevailing northwestern winds (Syberian) in winter, it has cold and dry weather with little rain. In contrast, the area is associated with the subtropical monsoon climate and has a hot and humid atmosphere with plenty of rain in summer. Because of the prevailing southeastern winds which carry marine air masses to the land, the region occasionally experiencing cyclones and typhoons. All of these lucrative conditions create an ideal bed to study and understand the impact of aerosols on cloud microphysics and assess their relation.

2.2. The MODIS sensor

The Moderate-resolution Imaging Spectroradiometer (MODIS) provides a comprehensive global observation of Earth's land, oceans, and atmosphere over 36 spectral channels from 0.41 to 14.235 µm at an altitude of 705 km, with a nadir spatial resolutions of 0.25 m (2 channels), 0.5 m (5 channels) and 1 km (29 channels) (Hu et al., 2018; Boiyo et al., 2018). A variety of aerosol and cloud properties were obtained from the MODIS Terra and Aqua satellites via continuous observations from 2000 and 2002, respectively. Terra's orbit around the Earth is timed so that it flies from the North to South across the equator in the morning (10:30 local time (LT)), while Aqua flies from south to north over the equator in the afternoon (13:30 LT). The MODIS instrument provides observations at moderate spatial (1-250 km) and temporal resolutions (1-2 days) over different portions of the electromagnetic spectrum. Recently, many studies have utilized the MODIS data products around the globe to understand the spatial heterogeneity in aerosol optical properties and discussed its data products, retrieval algorithms, calibration, and uncertainties (He et al., 2016; Hu et al., 2018; Boiyo et al., 2018; Kumar et al., 2018). Data products of aerosol and cloud are among the hundreds of products of measured radiance derived from the MODIS (Dahutia et al., 2017). Two significant new approaches to AOD retrieval algorithms have been introduced: the Dark Target (DT) and Deep Blue (DB). The first approach involves the DT retrieval best suits over land and ocean surfaces, which is limited to surface reflectance up to 0.15 and assumes transparency of aerosols in the mid-IR spectral range (Remer et al., 2005; Levy et al., 2007, 2013). The second approach involves the DB algorithm, which differs much compared to the DT (Sayer et al., 2013). As the primary concern related to low reflectance, the blue part of the visible region is more prominent than in the red component. It is used to retrieve aerosol products for geographical areas with surface reflectance greater than 0.15. However, the DB algorithm decreases the influence of albedo effects over bright surfaces, and has high accuracy over land, except over dust and snow surfaces.

Since Terra and Aqua have different overpass times, we have used data from the MODIS-Terra satellite to investigate the spatiotemporal patterns and relationship between aerosol and cloud properties. The Terra-MODIS Collection 6.0 level-3 combined/merged (DTB) daily aerosol and cloud products were downloaded from the GIOVANNI over East China from 2000 to 2017. The detailed information on algorithms for the retrieval of aerosol data products is available at https://giovanni.sci.gsfc.nasa.gov/giovanni/. The estimated uncertainty in the MODIS AOD product was reported as 0.03 ± 0.15 and 0.05 ± 0.20 over the ocean and land, respectively (Tanre et al., 1997; Kaufman et al., 1997). Recently, the Collection 6.1 DT and DB products are released and modified several products over the land and ocean surfaces, compared to the earlier Collection 6.0. The use of data with 1°×1° resolution (aerosol and cloud parameters) allows us to reduce the uncertainty induced by each Level-2 pixel. In particular, we have used collocated data of aerosol and cloud products such as AOD_{550} (Unitless), Water Vapor (WV, cm), Cloud Fraction (CF, Unitless), Cloud effective radius (CER, micron), Cloud Top Pressure (CTP, hPa) and Cloud Top Temperature (CTT, K).

2.3. Statistical methods

The linear regression statistical approach is capable of quantifying and statistically estimating the trends of long-term data for a particular geophysical variable. In the present study, the same technique was adopted for the annual and seasonal trend analyses in AOD alongside for the meteorological parameters. The method has previously been used in other related studies (Kumar et al., 2014, 2018; Kang et al., 2016; Boiyo et al., 2018) has a practical usage of directly quantifying the direction and magnitude of the trend in t data. Following this method, a linear trend model (Eq. 1) was adopted:

$$Y_t = c + \omega * X_t + \varepsilon \tag{1}$$

where Y_t c and X_t represent the geophysical variable, c is the offset (y-intercept), and X_t is the independent variable representing time, respectively. However, ω is the trend estimate of the Y_t under consideration, while ε is the noise in the time series. The statistical significance of the estimated trends was further tested using the method developed by Weatherhead et al. (1998). Adding to this, the patterns are considered significant with a p-value of 0.05 or a 95% confidence interval when $\left|\frac{\omega}{\delta}\right|$ > 2, whereas trends are considered significant at a 90% confidence level when 1.5 < $\left|\frac{\omega}{\delta}\right|$ < 2; here δ define the standard deviation of the slope affiliated with the linear regression.

The relative change in AOD (which relates the current with initial AOD values) can be used to describe the inter-annual variations in AOD quantitatively. In the present work, the annual and seasonal relative changes in AOD (in decimal form) are computed using the expression:

$$\text{Relative AOD Change}_{\text{a(s)}} = \frac{\text{Average AOD }(2009-2016)_{\text{a(s)}} - \text{Average AOD }(2002-2008)_{\text{a(s)}}}{\text{Average AOD }(2002-2008)_{\text{a(s)}}} \tag{2}$$

where subscripts ‘a’ and ‘s’ denote annual and seasonal AOD values, respectively.

3. Results and discussion

3.1. Spatial and temporal changes of AOD

3.1.1. Spatial distributions

The spatial distribution of mean yearly AOD_{550} found that the 18-year climatology of aerosols had a marked impact on the study domain (Fig. 2). It is showed that the AOD gradual increase from the South to the North of the study domain (Fig. 2a). There is an apparent north-south demarcation line that means the Qinling Mountains-Huaihe line (QHL), which is called the geographical dividing line between the South and the Northern parts of East China. Further, there are significant differences observed between the South and North of the study area in terms of the amount of vegetation, precipitation, annual average temperature, or geographical features. Also, the rain found in the South of QHL (Fig. 1c) was much higher due to the subtropical monsoon climate leads to a higher normalized differential vegetation index (NDVI) (Fig. 1b) over the entire study domain.

High AOD (>0.8) (Fig. 2b) was noticed in the North of the study domain (over the western Shandong province) surrounded with high population density and intense anthropogenic activities resulting in a significant accumulation of fine-mode particles with moderate to high values of AE (1.1-1.3) (Fig. 2b). Although, the Shandong province is characterized by lower urbanization compared with the Yangtze River Delta (YRD), and is susceptible to windblown dust particles transported from the North region round the year (Yu et al., 2016). Also, high AOD is possibly due to the aerosols produced from industrial sectors like coal-fired power stations, petrochemical operations, and frequent construction activities (due to rapid urbanization), over this region, contributed to the observed high AOD. Apart, high AOD (> 0.8) and low AE (< 1.0) were evidenced over Shanghai Municipal Corporation, which is a heavily polluted city situated close to the marine environment enriched with coarse salt particles. Moderate AOD values (0.4–0.7) were depicted in the central parts of East China, where the areas of Jiangsu and Anhui provinces and Shanghai cities are located. While low AOD between 0.1 and 0.3 and high AE values (> 1.4) were observed in the southern regions (Jiangxi, Fujian, and Zhejiang provinces) of the study domain are highly vegetated (large NDVI) with more amount of rain rate (Fig. 1c). From the reasons as mentioned earlier, it is now clear to some extent that, the AOD in China, mainly East China is closely related to the growing population, topography, meteorological changes, and climate, for aerosol distribution, which is comparable with the results reported by Luo et al. (2014), Hu et al. (2018) and He et al. (2016) using the long-term MODIS data.

Figs. 3a-d presents the spatial distribution of seasonal mean AOD_{550} with maximum (> 1.0) noticed in summer and minimum in winter (< 0.1). The highest AOD appeared in the urban areas of Shandong province with dense population and thriving industries. At the same time, the lowest AOD was found almost around the year in the southern regions of the study domain. Several investigators have also reported the persistence of high AOD during summer over the area (Hu et al., 2018; He et al., 2016). However, the seasonal AE values over the study domain were found 1.4 (Figs. 3e-h), except spring indicates the dominance of fine-mode aerosols. The low AE (0.6) found over Jiangxi, Fujian, and Zhejiang provinces during the spring denote that aerosols in those areas are large (coarse) particles originating from the desert regions.

3.1.2. Temporal variations

The inter-annual monthly and seasonal mean changes of AOD_{550} along with the standard deviation obtained from the daily values during 2000 - 2017 for the selected eight cities are shown in Table 2 and Fig. S1 of Supplementary Material (SM). It is inferred that AOD showed a persistent deviation with lower values, which occurred during December (winter) in most areas of the study domain, except for the smaller latitude locations (NC, FZ, and XM), where the AOD was found lower in July. However, the AOD peaks during June (summer) in most of the areas, except for NC, FZ, and XM, where it was found maximum during April with large standard deviations, indicate large variability in the individual daily AOD values. Whereas, the profound differences were found during the spring represent more stability in the AOD values, except for FZ and XM sites with low amounts of standard deviations in autumn. In association with anthropogenic and natural sources, on average, low and high AOD values of 0.19±0.12 and 1.29±0.38 were noticed at FZ (in December) and JN (in July) for the entire period of study in East China (Table 2). The reason behind this abrupt seasonality attributed to the fact that these are mostly industrial, low vegetation coverage, and effective biomass burning regions (He et al., 2016; Hu et al., 2018). Further, the dust transported coarse particles from the northeast arid domain during late spring is also the leading cause of increasing AOD values in summer at the study sites.

Kumar (2014), Alam et al. (2010, 2014), and Sharif et al. (2015) concluded that water vapor (precipitate) and AOD are directly related to each other. Hence, a higher concentration of water vapor in summer leads to a higher AOD. Besides, higher air temperatures tend to hold more water vapor that feeds gas-to-particle conversion mechanism, which might be the other reason causing the higher AOD levels in the summertime (Kang et al., 2016; Hu et al., 2018). During the winter season, the AOD found low values for all stations over the study domain likely related to low water vapor content in the atmosphere that restricts the possibility of the hygroscopic growth of aerosols (Pan et al., 2010; Khan et al., 2019). Moreover, the dynamics played by the planetary boundary layer, which is higher in summer than winter resulting in significant diffusion of aerosols, leads to lower AOD in winter (Kang et al., 2020; Shao et al., 2020). Several authors found similar results over China in the recent past (Yuan et al., 2008; Gao et al., 2014, and references therein). However, in our case, it deviates from season to season due to regional anthropogenic and natural pollution (Pan et al., 2010; He et al., 2012; Hu et al., 2018; Shao et al., 2020).

3.2. Spatial tendencies in aerosol optical properties

The spatial trends obtained on the annual and seasonal indices using the observed daily AOD and AE datasets over East China during 2000-2017 are presented in Figs. 4 and 5. The yearly mean spatial tendencies of AOD_{550} were noticed positive (>0.013) with the relative trend of ~0.02 over the urban-industrialized regions of the North, East, and Northwest of the study domain. While the lowest negative trend (< -0.01) was associated with the rural and less developed areas of the South and Southwest of the domain, the positive trend in AOD implies an increase in aerosol load, attributed to the extensive anthropogenic activities, and urban development. Further, an increasing trend in AE indicates the dominance of fine-mode particles over the region. The seasonal-based spatial pattern is more widespread in AOD as compared to the AE parameter over the study domain. Similarly, the seasonal trends having high AOD with corresponding high AE were characterized over the economically industrial regions of the central and north of the study domain during most of the study period, being more pronounced in the autumn season. However, the decreasing trends (< −0.01) were found in southern regions of East China ascribed to an increase of coarse-mode particles originating from the natural sources. Further, the decreasing tendencies in AOD and AE during summer was observed in the northern parts of the study domain (over the western Shandong province), denotes the dominance of coarse-mode particles due to dust aerosols coming from the deserts (Taklimakan and Mongolia), with the prominence of sea salt aerosols from the East and South of China Sea. These results are consistent, and agreement with the previous investigations observed over entire China (Luo et al., 2014; Kang et al., 2016; Hu et al., 2018; Shao et al., 2020).

3.3. Spatiotemporal changes in cloud parameters

The spatial (Fig. 6) and temporal (Fig. 7 and Table 3) distributions of different cloud parameters (COT, CF, CER, CTT, and CTP) over East China were analyzed using the long-term (2000 to 2017) MODIS Terra satellite data. The annual spatial changes and the time sequence variation in the COT are significant between the southern and northern parts of the study domain (Figs. 6b and 7b). The mean COT in the southwest and southern regions was the highest during February. However, the spatial distribution is just the opposite in the northern domain because annual average moisture content and temperature are lower in the North than in the South of the study domain; and the clouds are relatively stable during winter months (Balakrishnaiah et al., 2012). The temporal variation shows that the COT over East China decreases first with time and gradually increases after 2004 with a maximum (~ 26) during November-December, and minimum (< 8) between September and October months, associated with general circulation, solar radiation, climate dynamics, and the amount of water vapor content in the atmosphere.

Fig. 6c shows a significant increase in cloud fraction (CF) over most parts of high elevation regions of Jiangxi, Fujian, and Zhejiang, with a large amount of CF (> 0.9) during February and March in East China (Fig. 7). This indicates more cloud cover over these sites. However, moderate mean CF values between 0.3-0.6 were noticed over the northern areas of the study domain. Kang et al. (2015) studied the spatial and temporal distributions of cloud parameters regionally over China using the long-term (2003-2013) data retrieved from Terra and Aqua MODIS cloud products and found more clouds over vegetated lands compared to coastal regions of East China.

Similarly, on the spatial and temporal scales, high values of CER were noted over north and middle regions (e.g., Jinan, Nanjing, and Hefei) with maximum values (17 µm) during June-August (summer) and minimum (12 µm) between December and February (winter) over southern parts of the study domain, respectively, attributed to the strong influence of dust and continental background aerosols (Figs. 6d and 7d). Fig. 6e shows the spatial distribution of CTT with higher values over southern regions of Fujian province, and lower at the Northwest of Shandong province. Similarly, the temporal variation indicates higher CTT values (267 K) during September-November (autumn) and lower (247 K) from April to June (spring) months, indicate the presence of cold clouds (<273 K) throughout the year in the study area, which is confirmed from the studies by Alam et al. (2014). Kumar (2014) and Sharif et al. (2015) pointed out an aerosol, as a critical player acting with clouds, changes not only the cloud properties (such as CF, CER, COT) but also affected the CTT and humidity profiles. Further, medium to lower values of CTP (550-630 hPa) was exhibited over the most parts of East China (Fig. 6f), except East, North, and Southern areas, where the mean CTP was recorded with its maximum (700 hPa) particularly, during November and December. Except for very small AOD over some areas, the CTP decreases with high cloud cover (CF), following the other studies reported over China (Tang et al., 2014; Gunaseelan et al., 2014). The highest WV value (5.5 cm) was recorded in July 2006 and August 2003 at the South and central areas of the study region, with the lowest (<1 cm) during the winter months in the North (Jinan), attributed to varying topography, seasonal variation in humidity profile, and meteorological factors (e.g., precipitation, temperature, and wind speed).

3.4. Spatiotemporal correlations between AOD and cloud parameters

In this section, the relationship between MODIS derived AOD and WV, and with cloud parameters such as COT, CF, CER, CTP, and CTT for the study domain has been discussed and presented individually through statistical correlation analysis for the period 2000–2017 in the following sections.

3.4.1. AOD and water vapor

The spatial correlation between AOD and WV revealed the positive relationship in most provinces over the study domain (Fig. 8); whereas, the negative spatial correlation was noticed over most areas in Anhui and Jiangsu provinces. Meanwhile, the strong positive correlations (0.6-0.8) were found in the northern part of Fujian and southern Zhejiang provinces. However, the relationship gradually weakens with an increase in latitude. It has been observed that the water-absorbing ability varies for different types of aerosols, with the dominance of sea salt aerosols in the South, and dust and soot particles in the remaining areas of China. The positive relations shows that the higher hygroscopic nature of aerosols and the negative relationship reveals that most of the local aerosols are commonly hydrophobic, including dust particles without coating by sulfate or other soluble inorganic and black carbon aerosols, attributed to different anthropogenic regional aerosols present in the atmosphere (Bhawar and Devara, 2010; Alam et al., 2014). The hygroscopic nature of aerosols, therefore, mainly depends upon the particular mixture of different types of particles as well as on the meteorological parameter (Kaufman et al., 2005). Besides, the cloud formation is also linked to hydrophilic aerosols in the presence of a sufficient amount of WV that will finally lead to changes in aerosol water uptake behavior and indirectly with the variation in both direct and indirect radiative forcing (Quass et al., 2010).

3.4.2. AOD and cloud optical thickness

The spatial correlation between AOD and COT (Fig. 8) showed a positive relation in the South of East China, where the AOD was commonly found lower; while going towards the northeast (urban regions of the study domain), it goes on increasing attributed to the same factors as discussed in the previous section. However, the maximum negative correlation was found between AOD and COT in most areas of the study domain, especially in the Eastern parts of Zhejiang province. The reason is that the regions are proximity to the coastal zone and are subject to sea and land breezes round the year (Guo et al., 2015), which is in good agreement with the investigations of Tang et al. (2014) and Kang et al. (2015) reported over East China. They suggested that environmental factors (such as meteorology (moisture) and radiative forcing present in the atmosphere) are also responsible key players, contributing to negative correlation. Sheng et al. (2019) and Kumar et al. (2018) reported that an increasing aerosol number concentration from anthropogenic sources is directly linked to variation in atmospheric humidity profiles that lead to the seasonal anomaly in the COT on the regional scale. Another possible reason is the presence of absorbing aerosols in the atmosphere, which causes a decrease in COT; and results in a negative correlation with AOD over Zhejiang province (Kang et al., 2015).

3.4.3. AOD and cloud fraction

The spatial correlation between AOD and CF over the study region for the period 2000–2017 is shown in Fig. 8. The decreasing trend between AOD and CF was found when the AOD value has reached below 0.4 over the Eastern Zhejiang. The results are consistent and agreement with the investigations of Kang et al. (2015) and Sheng et al. (2019) over China, Kumar (2014) over India, Adesina et al. (2016) over South Africa, and Kumar et al. (2018) over Kazakhstan. No apparent correlations were found between AOD and CF for most of the areas in Fujian and Jiangxi regions. The maximum positive relationship between AOD and CF was found in the areas of the southern part of Shandong province due to more aerosol particles from urban, industrial, and domestic anthropogenic activities. It is also important to mention that the substantial increase in CF with AOD in those regions having high aerosol concentration, which is relatively hydrophobic, such as biomass burning and dust aerosols (Kumar, 2014).

However, those areas which are under the influence of low atmospheric pressure have noticed in more tendencies to create conditions necessary for cloud formation by accumulating aerosol particles and WV cause coarse-mode aerosols tend to form CNN (Bhawar and Devara, 2010). Hence, the maximum positive correlation was noticed between the parameters AOD and CF in the southern Shandong region. Myhre et al. (2007) and Kaufman et al. (2005) had identified a strong correlation between CF, relative humidity, and vertical velocity, indicating that the relationship is strongly affected by the meteorological factors. However, the CF exhibits a weak negative correlation (Fig. 9) with the potential temperature lapse rate, relative humidity, and vertical shear of the horizontal wind in the middle atmosphere. Overall, the significant relationship between AOD and CF over the entire study domain, except the low correlation in the north is related to the impact of meteorological factors interlink with the aerosol transport, the type of land surface (albedo), and the complexity of the study domain (Balakrishnaiah et al., 2012).

3.4.4. AOD and cloud effective radius

The spatial correlation between CER and AOD depicted negatively over a small area (Fig. 8), and the rest are positively correlated over East China. It is revealed that the positive correlation occurred between AOD and CER only when the AOD is higher than 0.4, which is an agreement with the findings of Tang et al. (2014) and Kang et al. (2015) over China and Kumar et al. (2018) over Kazakhstan. Kaufman et al. (2005) had reported a reverse tendency of CER versus AOD over the Atlantic Ocean. Adding, Tang et al. (2014) also noticed similar negative results for AOD and CER over the open oceanic regions in the East part of China. Besides, the maximum positive correlation coefficient was obtained mainly from the southern Shandong province due to the coarse-mode aerosols resulting from the transport of dust particles. However, the aerosols are dominated by fine particles in the southern part of the study area, with a sufficient amount of water vapor that would increase the chance of particles hitting and blending, leading to the positive correlation between AOD and CER. Furthermore, the positive correlation between AOD and CER (Fig. 9) was observed mainly associated with different processes such as microphysical and dynamical effects that are likely counteracting the indirect effect of aerosols on cloud droplets, which is defined as the well-known "Twomey effect." Yuan et al. (2008) and Kumar et al. (2018) also revealed positive correlations between AOD and CER over the study area, which they interlinked with the effects of soluble organic particles and giant cloud condensation nuclei (CCN). They added that such particles have the tendency to contribute the most to large AOD but fewer total cloud droplets and thus lead to higher CER.

3.4.5. AOD and cloud top temperature

The spatial correlation between AOD and CTT during the period of study for the entire study domain is shown in Fig. 8. The CTT showed an inverse tendency concerning the AOD parameter (negative correlation) in the Northern part of the study area because the CTT was found to remain insensitive for the changes in aerosol number concentration. This particular behavior of CTT may be possible because the aerosols acting on clouds change their properties like COT, CTT, and cloud cover. However, the CTT showed a positive tendency with AOD (Fig. 9) in the rest of the study regions likely due to large-scale meteorological changes, including complex interplay among convection activities, dynamics of the PBL, and cloud parameterizations in those regions (Yuan et al., 2008).

3.4.6. AOD and cloud top pressure

The spatial correlation between AOD and CTP over the study area during 2000-2017 is shown in Fig. 8f. A negative correlation between CTP and AOD was observed over most parts of the study domain. Previous studies by Alam et al. (2014) and Kumar et al. (2018) have reported that, except for some regions of lower AOD, CTP was mainly found in reverse pattern with AOD in most of the areas, especially in higher cloud altitude regions. The same is resulted from the suppression of the precipitation by an increasing cloud lifetime and thus, also affecting the cloud albedo and changing the CTP (Balakrishnaiah et al., 2012). Kaufman et al. (2005) and Lee and Penner (2011) have reported that the CTP decreases with an increase of AOD because an increasing CER leads to decreasing CTP. The observation supports that the CF increases with an increase in AOD, while CTP decreases with CF (Fig. 9). Koren et al. (2008) and Kumar et al. (2018) suggested that all these vertical winds of the region are strongly correlated with the changing CTP and CF. The vertical wind velocity is the most important meteorological parameter influencing the cloud properties. All these variations suggest an association between meteorology and aerosol in these regions.

3.5. Linear trends in aerosol and cloud parameters

To characterize the aerosol and clouds optical parameters, the inter-annual (Fig. 10 and Table 4) and seasonal (Table 5) variability on time series and trend analysis were performed during the entire study period over East China. The AOD (2.03%), CF (0.42%), and CER (0.06%) exhibited an increasing trend in all seasons, whereas, the CER showed a converse in DJF. The annual and seasonal (DJF, SON) percentage increase in AOD trends (positive slope) is significant at 99% confidence level, and the rest of the seasons showed 90% confidence (Fig. 10 and Table 5). Furthermore, an increasing tendency in AOD is generally attributed to the continuous increase in population, industrialization, and source emissions over the study area. The decrease (increase) in CER (CF) with AOD is following the classical theory (Twomey, 1977). However, the COT and CTT decreases with AOD associated with the fact that the CER increases with a decrease in CTP, as illustrated by Myhre et al. (2007), Gunaseelan et al. (2014) and Alam et al. (2014).

On the other hand, the decrease in annual trend in CTP (-0.59%), COT (-0.06%), and CTT (-0.07%) is associated with the changes in meteorological condition and source emissions at the study area. Meanwhile, the WV passed the significant test at a 99% confidence level, decreasing with ~0.35% per year, being the highest with 0.03% during JJA (Tables 4, 5). The above is attributed to hygroscopic phenomena, biomass burning, and change in atmospheric dynamics, and is consistent with the observations on trends in CTT and CTP. Though the trend of variations in these parameters is more/less considerable, in general rule, the meteorological conditions have a substantial impact on the relationship between AOD and WV (Balakrishnaiah et al., 2012).

The annual mean distribution of aerosol and cloud parameters during 2000-2017 revealed distinct features with mean (±SD) AOD, (0.69±0.48), COT (15.54±3.21), CF (0.72±0.05), CER (14.65±1.03 micron), CTT (258.15±3.58 K) and CTP (609.84±109.6 hPa) values, being highest in the year 2000 for COT (18.43), CTP (680 hPa) and CTT (261 K). The highest values of the CF approach to 0.76 for the year 2012, followed by 2015 (0.75) and the lowest CF (0.66) in the year 2004. Further, the detailed statistical matrices are given in Tables 4 and 5, presenting their mean, standard deviation, slope, trend, and p-value on a seasonal and annual basis for the entire study period. An increase in AOD over East China corresponds to a decrease in CTP and an indirect increase in COT values, following the finding of Kang et al. (2015) and Tang et al. (2014). The same will have an impact on the formation and growth of aerosols and clouds over the study region. However, CF increase with AOD is relatively independent of aerosol chemical composition but is relevant to the particle-size towards the CCN mechanism (Bhawar and Devara, 2010).

5. Summary of conclusions

Atmospheric aerosols are one of the key players influencing the clouds mechanism and radiative forcing in multiple ways. However, the role of aerosols in modifying the clouds has been one of the most intriguing questions in the world of clouds and the study of climate change. The spatial gradient of AOD_{550} showed an increase from the South to the Northern parts of the study area. The maximum AOD attributed to large population density, enhanced anthropogenic activities, and dominance of coarse dust particles transported from the North China region. Whereas the low AOD_{550} may be related to highly NDVI areas with high precipitation rate, and favorable meteorological conditions resulted in the suspension of particles. The higher concentration of aerosols in summer is due to the higher amount of water vapor, higher temperature, and relative humidity, which are helpful to gas-to-particle conversion mechanism. Furthermore, there are significant increasing trends in AOD values over Shandong, due to increasing urban activities, and use of fossil fuels and biomass burning emissions

The spatial correlations of AOD with cloud parameters provides a better understanding of aerosol-cloud properties relation based on the analysis of positive and negative correlation values over the study domain. In the present study, the spatial correlation between AOD and WV was found negative over most areas in Anhui and Jiangsu, cause the water-absorbing ability of different types of aerosols is unusual. We also found that the correlation between AOD and CER is positive over most of the study sites, due to the coarse-mode aerosols resulting from dust and burning particles over the north of the study domain. Another reason is that sufficient water vapor would increase the chance of particles hitting and blending, leading to a positive correlation between AOD and CER. And then, the growth of CER facilitates the formation of CNN, leading to a positive relationship between AOD and CF over most of the study area. The spatial correlations between AOD and CTP, CTT are similar; in general, they have noticed a negative correlation. The reason is that an increasing CER leads to decreasing CTP, and CTT were found to remain insensitive for the changes in aerosol number concentration.

The linear trend analysis conducted over the annual mean values of different aerosol and cloud parameters showed an increasing trend in AOD, CER, and CF and decreasing patterns of WV, CF, CTT, and CTP. Over the northern regions (Shandong province), the positive correlation between CER, AOD, and CTT was found for most of the years attributed to meteorological changes; whereas, the negative relationship is evident over the coastal regions.

Appendix A. Supplementary data

Supplementary data to this article can be found online at http://dx.doi.org/10.1016/j.atmosenviron.xxxx.xx.xxx.

CRediT author statement:

All authors have read and agreed to the published version of the manuscript.

Jing Huang: Conceptualization, Formal analysis, Investigation, Visualization, Writing-original draft preparation. **Lingbing Bu:** Supervision, Funding Acquisition, Project Administration, Writing-review and editing. **Kanike Raghavendra Kumar:** Conceptualization, Investigation, Resources, Writing-review and editing. **Rehana Khan:** Data curation, Writing-review and editing. **N.S.M.P. Latha Devi:** Data curation, Language editing, and formatting.

Funding Sources: This research work is supported by the National Natural Science Foundation of China (Grant Nos. 91644224, 41775123). The authors KRK and NSMPLD are grateful to the Department of Science and Technology (DST), Government of India, for the award of DST-FIST Level-1 (SR/FST/PS-1/2018/35) scheme to Department of Physics, KLEF.

Acknowledgments: We acknowledge the MODIS and TRMM scientific data team for providing and processing various satellite datasets used in this study and to the NCEP/NCAR for providing reanalysis meteorological datasets. The authors would like to acknowledge Prof. James J. Schauer, Editor-in-Chief and Prof. Zhengqiang Li, Associate Editor of the Journal, and the two anonymous reviewers for their helpful comments and constructive suggestions towards the improvement of earlier versions of the manuscript.

Data Availability Statement: The data that support the findings of this study are available open and free to the public and can be downloaded from Giovanni at https://giovanni.sci.gsfc.nasa.gov/giovanni/.

Conflicts of Interest: The authors declare that they have no conflicts of interest.

References

Ackerman, A.S.; Toon, O.B.; Stevens, D.E.; Heymsfield, A.J; Ramanathan, V. Reduction of tropical cloudiness by soot. Science 2000, 288, 1042–1047.

Adesina, A.J.; Kumar, K.R.; Sivakumar, V. Aerosol-cloud-precipitation interactions over major cities in South Africa: Impact on regional environment and climate change. Aerosol Air Qual. Res. 2016, 16, 195-211.

Alam, K.; Iqbal, J.; Blaschke, T.; Qureshi, S.; Khan, G. Monitoring spatio-temporal variations in aerosols and aerosol cloud interaction over Pakistan using MODIS data. Adv. Space. Res. 2010, 46, 1162–1176.

Alam, K.; Khan, R.; Blaschke, T.; Mukhtiar, A. Variability of aerosol optical depth and their impact on cloud properties in Pakistan. J. Atmos. Sol. Terr. Phys. 2014, 107, 104-112.

Balakrishnaiah, G.; Kumar, K.R.; Reddy, B.S.K.; Gopal, K.R.; Reddy, R.R.; Reddy, L.S.S.; Babu, S.S. Spatio-temporal variations in aerosol optical and cloud parameters over southern India retrieved from MODIS satellite data. Atmos. Environ. 2012, 47, 435–445.

Bao, S.; Letu, H.; Zhao, J.; Lei, Y.; Zhao, C.; Li, J.; Tana, G.; Liu, C.; Guo, E.; Zhang, J.; He, J.; Bao, Y. Spatiotemporal distributions of cloud radiative forcing and response to cloud parameters over the Mongolian Plateau during 2003-2017. Int. J. Climat. 2020, doi:10.1002/joc.6444.

Bao, S.; Letu, H.; Zhao, J.; Shang, H.; Lei, Y.; Duan, A.; Chen, B.; Bao, Y.; He, J. Spatiotemporal distributions of cloud parameters and their response to meteorological factors over the Tibetan Plateau during 2003-2015 based on MODIS data. Int. J. Climat. 2019, 39, 532-543.

Bhawar, R.L.; Devara, P.C.S. Study of successive contrasting monsoon (2001-2002) in terms of aerosol variability over tropical station Pune, India. Atmos. Chem. Phys. 2010, 10: 29–37.

Boiyo, R.; Kumar, K.R.; Zhao, T. Spatial variations and trends in AOD climatology over East Africa during 2001–2015: A comparative study using three satellite datasets. Int. J. Climatology. 2018, 38 (S1), 1221-1240.

Dahutia, P.; Pathak, B.; Bhuyan, P.K. Aerosols characteristics, trends and their climatic implications over Northeast India and adjoining South Asia. Int. J. Climat. 2017, 38, 1234-1256

Dey, S.; di Girolamo, L. A climatology of aerosol optical and microphysical properties over the Indian subcontinent from9 years (2000-2008) of Multiangle Imaging Spectroradiometer (MISR) data. J Geophys Res. 2010, 115: 15204.

Gunaseelan, I.; Bhaskar, B.V.; Muthuchelian, K. The effect of aerosol optical depth on rainfall with reference to meteorology over metro cities in India. Environ. Sci. Pollut. Res. 2014, 8188-8197.

Guo, X.; Fu, D.; Guo, X.; Zhang, C. A case study of aerosol impacts on summer convective clouds and precipitation over northern China. Atmos. Res. 2014, 142, 142–157.

He, Q.; Li, C.; Geng, F.; Lei, G.; Li, Y. Study on long-term aerosol distribution over the land of East China using MODIS data. Aero. Air Qual. Res. 2012, 12, 304–319.

He, Q.; Zhang, M.; Huang, B. Spatio-Temporal Variation and Impact Factors Analysis of Satellite-Based Aerosol Optical Depth over China from 2002 to 2015. Atmos. Environ. 2016, 129, 79–90.

Hu, K.; Kumar, K.R.; Kang, N.; Boiyo, R.; Wu, J. Spatial-temporal characteristics of aerosols and changes in trends over China with recent MODIS Collection 6 satellite data. Environ Sci Pollut Res. 2018, 25, 6909-6927.

IPCC. Climate Change 2013: The Physical Science Basis. Contribution of Working Group I to the Fifth 4 Assessment Report of the Intergovernmental Panel on Climate Change [Stocker, T. F., D. Qin, G.-K.5 Plattner, M. Tignor, S. K. Allen, J. Boschung, A. Nauels,Y. Xia, V. Bex and P. M. Midgley (Eds.)].6 Cambridge University Press, Cambridge, United Kingdom And New York, NY, USA, 2013, 1535.

Kang, N.; Deng, F.; Khan, R.; Kumar, K.R.; Hu, K.; Yu, X.; Wang, X.; Latha, D.N.S.M.P. Temporal variations of PM concentrations, and its association with AOD and meteorology observed in Nanjing during the autumn and winter seasons of 2014-2017. J. Atmos. Sol. Terr. Phys. 2020, 203, 105273.

Kang, N.; Kumar, K.R.; Yin, Y.; Diao, Y.; Yu, X. Correlation analysis between AOD and cloud parameters to study their relationship over China using MODIS data (2003-2013): Impact on cloud formation and climate change. Aerosol Air Qual. Res. 2015, 15, 958-973.

Kang, N.; Kumar, K.R.; Kang, H.; Xingna Y.; Yan Y. Long-Term (2002 – 2014) Evolution and Trend in Collection 5.1 Level-2 Aerosol Products Derived from the MODIS and MISR Sensors over the Chinese Yangtze River Delta. Atmos. Res. 2016, 181, 29–43.

Kaufman, Y.J.; Fraser, R.S. The effect of smoke particles on clouds and climate forcing. Sci. 1997, 277, 1636–1639.

Kaufman, Y.J.; Koren, I.; Remer, L.A.; Rosenfeld, D.; Rudich, Y. The effect of smoke, dust, and pollution aerosol on shallow cloud development over the Atlantic Ocean. Proc. Natl. Acad. Sci. 2005, 102, 11207–11212.

Khan, R.; Kumar, K. R.; Zhao, T. The climatology of aerosol optical thickness and radiative effects in Southeast Asia from 18-years of ground-based observations. Environ. Pollut. 2019, 254, 113025.

Koren, I.; Martin, J.V.; Remer, L.A.; Afargan, H. Smoke invigoration versus inhibition of clouds over the Amazon. Sci. 2008, 321, 946-949.

Kumar, A. Long term (2003-2012) spatio-temporal MODIS (Terra/Aqua level 3) derived climatic variations of aerosol optical depth and cloud properties over a semi arid urban tropical region of Northern India. Atmos. Environ. 2014, 83, 291–300.

Kumar, K.R.; Boiyo, R.; Madina, A.; Kang, N. A 13-year climatological study on the variations of aerosol and cloud properties over Kazakhstan from remotely sensed satellite observations. J. Atmos. Sol. Terr. Phys. 2018, 179, 55-68.

Kumar, K.R.; Sivakumar, V.; Yan Y.; Reddy, R.R.; Kang, Na.; Yiwei D.; Adesina, A.J.; Xingna Y. Long-Term (2003-2013) Climatological Trends and Variations in Aerosol Optical Parameters Retrieved from MODIS over Three Stations in South Africa. Atmos. Environ. 2014, 95, 400–408.

Lee, S.S.; Penner, J.E. Dependence of aerosol-cloud interactions in stratocumulus clouds on liquid-water path. Atmos. Environ. 2011, 45, 6337–6346.

Levy, R.C.; Lorraine, A.R.; Shana, M.; Eric, F.; Vermote.; Kaufman, Y.J. Second-Generation Operational Algorithm: Retrieval of Aerosol Properties over Land from Inversion of Moderate Resolution Imaging Spectroradiometer Spectral Reflectance. J.Geophys.Res. 2007, 112, 1–21.

Levy, R.C.; Mattoo, S.; Munchak, L.A.; Remer, L.A.; Sayer, A.M.; Patadia, F.; Hsu, N.C. The Collection 6 MODIS aerosol products over land and ocean. Atmos. Meas. Tech. 2013, 6, 2989-3034.

Li, B.; Yuan, H.; Niu, F.; Tao, S. Spatial and temporal variations of aerosol optical depth in China during the period from 2003 to 2006. Int. J. Rem. Sens. 2010, 31, 1801–1817.

Luo, Y.; Zheng, X.; Zhao, T.; Chen, J. A climatology of aerosol optical depth over China from recent 10 years of MODIS remote sensing data. Int. J. Climat. 2014, 34, 863-870.

Myhre, G.; Stordal, F.; Johnsrud, M.; Kaufman, Y.J.; Rosenfeld, D.; Storelvmo, T. Aerosol-Cloud interaction inferred from MODIS satellite data and global aerosol models. Atmos. Chem. Phys. 2007, 7, 3081-3101.

Pan, L.; Che, H.Z.; Geng, F.H.; Xia, X.G.; Wang, Y.Q.; Zhu, C.Z.; Chen, M.; Gao, W.; Guo, J.P. Aerosol optical properties based on ground measurements over the Chinese Yangtze Delta region. Atmos. Environ. 2010, 44, 2587–2596.

Qin, Y.; Liu, Y.; Wang, L.; Lin , A.; Xia, X.; Che, H.; Bilal, M.; Zhang, M. Characteristics and driving factors of aerosol optical depth over Mainland China during 1980-2017. Remote Sens. 2018, 10, 1064,

Quass, J.; Stevens, B.; Stier, P.; Lohmann, U. Interpreting the cloud cover aerosol optical depth relationship found in satellite data using a general circulation model. Atmos. Chem. Phys. 2010, 10, 6129–6135.

Remer, L.A.; Kaufman, Y.J.; Tanre, D.; Matoo, S.; Chu, D.A.; Martins, J.V.; Li, R.R.; Ichoku, C.; Levy, R.C.; Kliedman, R.G.; Eck, T.F.; Vermote, E.; Holben, B.N. The MODIS aerosol algorithm, products and validation. J. Atmos. Sci. 2005, 62, 947–973.

Saud, T.; Dey, S.; Das, S.; Dutta, S. A satellite-based 13-year climatology of net cloud radiative forcing over the Indian monsoon region. Atmos. Res. 2016, 182, 76-86.

Sayer, A.M.; Hsu, N.C.; Bettenhausen, C.; Jeong, M.J. Validation and uncertainty estimates for MODIS Collection 6 "deep Blue" aerosol data. J. Geophys. Res. Atmos. 2013, 118(14), 7864-7872.

Shao, J.; Yi, F.; Yin, Z. Aerosol leyers in the free troposphere and their seasonal variations as observed in Wuhan, China. Atmos Environ. 2020, 117323.

Sharif, F.; Alam, K.; Afsar, S. Spatio-temporal distribution of aerosol and cloud properties over Sindh using MODIS satellite data and a HYSPLIT model. Aerosol Air Qual. Res. 2015, 15(2): 657-672.

Sheng, Z.; Liu, C.; Zhang, X. Spatial and temporal distribution of the cloud optical depth over China based on MODIS satellite data during 2003–2016. J. Environ. Sci. 2019, 80, 66 – 81.

Tang, J.; Wang, P.; Mickley, L.J.; Xia, X.; Liao, H.; Yue, X.; Sun, L.; Xia, J. Positive relationship between liquid cloud droplet effective radius and aerosol optical depth over Eastern China from satellite data. Atmos. Environ. 2014, 84, 244–253.

Tanré, D.; Kaufman, Y.J.; Herman, M.; Mattoo, S. Remote Sensing of Aerosol Properties over Oceans Using the MODIS/EOS Spectral Radiances. J.Geophys.Res. 1997, 102, 16971.

Torres, O.; Bhartia, P.K.; Herman, J.R.; Ahmad, Z.; Gleason, J. Derivation of aerosol properties from satellite measurements of backscattered ultraviolet radiation: Theoretical basis. J.Geophys.Res. 1998, 103, 17099–17110.

Twomey, S. Influence of Pollution on Shortwave Albedo of Clouds. J. Atmos. Sci. 1977, 34, 1149–1152.

Wang, Y.; Chen, L.; Xin, J.; Wang, X. Impact of the dust aerosol model on the VIIRS aerosol optical depth (AOD) product across China. Remote Sens. 2020, 12, 991.

Weatherhead, E.C.; Gregory, C.; Reinsel, G.C.; Tiao, X.L.M.; Dongseok, C.; Wai, K.C.; Teddie, K. Factors Affecting the Detection of Trends: Statistical Considerations and Applications to Environmental Data. J.Geophys.Res. 1998, 103 (D14), 17149.

Yu, X.; Lu, R.; Kumar, K.R.; Ma, J.; Zhang, Q.; Jiang, Y.; Kang, N.; Yang, S.; Wang, J.; Li, M. Dust aerosol properties and radiative forcing observed in spring during 2001–2014 over urban Beijing, China. Environ. Sci. Pollut. Res. 2016, 23, 15432-15442.

Yuan, T.L.; Li, Z.Q.; Zhang, R.Y; Fan, J.W. Increase of cloud droplet size with aerosol optical depth: an observation and modeling study. J. Geophys. Res. 2008, 113.

Table 1. Geographical information about the selected regions of study in East China.

S. No.	Region/Capital city	Province	Latitude (N)	Longitude (E)	Altitude ASL (m)	Population (~million)	Area (km^2)	Atmospheric pressure (KPa)
1	Jinan (JN)	Shandong	36°40′	116°59′	51	6.3	8,177	99.85
2	Hefei (HF)	Anhui	31°52′	117°17′	30	7.3	11,408	100.09
3	Nanjing (NJ)	Jiangsu	32°03′	118°46′	9	6.6	6,501	100.4
4	Shanghai (SH)	Shanghai city	31°14′	121°29′	5	14.5	6,340	100.53
5	Hangzhou (HZ)	Zhejiang	30°16′	120°10′	42	7.4	16,596	100.05
6	Nanchang (NC)	Jiangxi	28°20′	115°55′	47	5.2	7,372	99.91
7	Fuzhou (FZ)	Fujian	26°05′	119°18′	84	6.9	12,153	99.64
8	Xiamen (XM)	Fujian	24°27′	118°06′	63	2.2	1,569	99.91

ASL-Above Sea Level. The population provided is according to the National Bureau of Statistics of the People's Republic of China by the end of 2016.

Table 2. Mean variations of AOD_{550} (± SD) over the selected cities in East China.

Month/ Season	Jinan (JN)	Hefei (HF)	Nanjing (NJ)	Shanghai (SH)	Hangzhou (HZ)	Nanchang (NC)	Fuzhou (FZ)	Xiamen (XM)
Jan	0.80±0.31	0.69±0.18	0.69±0.16	0.64±0.14	0.46±0.16	0.72±0.28	0.22±0.09	0.29±0.08
Feb	0.93±0.28	0.77±0.21	0.75±0.20	0.66±0.19	0.44±0.11	0.67±0.29	0.23±0.07	0.30±0.11
Mar	0.78±0.12	0.69±0.15	0.69±0.13	0.60±0.10	0.48±0.10	0.56±0.10	0.34±0.10	0.37±0.14
Apr	0.66±0.09	0.56±0.09	0.57±0.07	0.55±0.12	0.46±0.12	0.59±0.16	0.36±0.11	0.37±0.17
May	0.58±0.19	0.62±0.14	0.63±0.11	0.59±0.14	0.45±0.13	0.53±0.12	0.28±0.21	0.34±0.12
Jun	1.25±0.22	1.20±0.41	1.24±0.32	1.01±0.43	0.70±0.31	0.71±0.41	0.28±0.11	0.26±0.19
Jul	1.29±0.38	0.62±0.31	0.75±0.27	0.55±0.26	0.38±0.15	0.38±0.19	0.20±0.07	0.25±0.12
Aug	0.94±0.31	0.63±0.27	0.70±0.28	0.57±0.35	0.45±0.18	0.54±0.26	0.20±0.06	0.27±0.33
Sep	0.74±0.22	0.50±0.18	0.55±0.21	0.46±0.20	0.54±0.21	0.52±0.17	0.23±0.06	0.32±0.24
Oct	0.82±0.22	0.63±0.15	0.64±0.15	0.48±0.11	0.47±0.20	0.55±0.19	0.25±0.09	0.28±0.07
Nov	0.64±0.14	0.55±0.13	0.59±0.08	0.55±0.12	0.39±0.13	0.53±0.19	0.22±0.11	0.23±0.05
Dec	0.60±0.16	0.53±0.16	0.57±0.19	0.52±0.14	0.40±0.19	0.51±0.13	0.19±0.12	0.22±0.09
Winter	0.78±0.30	0.66±0.21	0.67±0.20	0.61±0.17	0.43±0.16	0.63±0.26	0.21±0.10	0.27±0.10
Spring	0.67±0.16	0.62±0.14	0.63±0.12	0.58±0.12	0.46±0.12	0.56±0.13	0.33±0.16	0.32±0.16
Summer	1.16±0.35	0.82±0.44	0.90±0.39	0.71±0.42	0.51±0.26	0.54±0.33	0.22±0.09	0.20±0.23
Autumn	0.73±0.21	0.56±0.17	0.59±0.16	0.50±0.16	0.46±0.19	0.53±0.19	0.24±0.09	0.27±0.15
Annual	0.84±0.33	0.67±0.28	0.70±0.26	0.60±0.26	0.47±0.19	0.57±0.24	0.25±0.12	0.27±0.17

Table 3. Temporal changes in aerosol and cloud properties during 2000–2017 over East China.

Month/ Season	AOD (unit less)	WV (cm)	COT (unit less)	CF (unit less)	CER (μm)	CTT (ºK)	CTP (hPa)
Jan	0.72±0.48	4.72±0.29	18.08±3.43	0.77±0.20	13.34±1.97	257.60±3.96	695.37±132.25
Feb	0.76±0.49	1.20±0.36	18.70±3.06	0.78±0.20	13.04±2.00	257.04±4.28	667.14±130.49
Mar	0.72±0.33	1.39±0.39	16.25±1.72	0.72±0.22	14.13±2.18	256.32±4.88	616.92±141.58
Apr	0.64±0.33	1.94±0.59	16.00±1.75	0.73±0.19	14.36±2.00	253.73±4.75	555.75±139.57
May	0.59±0.36	2.76±0.75	15.83±1.37	0.74±0.19	14.99±1.95	253.42±4.49	517.26±130.73
Jun	1.08±0.60	3.74±0.85	14.93±0.83	0.79±0.15	15.74±1.58	253.96±4.55	467.22±113.81
Jul	0.75±0.63	4.79±0.64	12.16±0.89	0.71±0.18	16.16±1.41	257.11±5.52	490.83±131.46
Aug	0.64±0.50	4.72±0.67	12.61±1.53	0.70±0.18	16.14±1.59	260.28±4.97	553.37±129.25
Sep	0.58±0.47	3.65±0.77	14.20±1.20	0.67±0.18	15.11±1.78	262.67±4.50	639.07±130.61
Oct	0.64±0.38	2.38±0.61	13.03±2.80	0.63±0.21	14.78±2.20	263.39±4.32	691.91±137.26
Nov	0.55±0.39	1.57±0.47	17.11±3.88	0.65±0.24	14.23±2.24	262.73±4.35	702.42±139.79
Dec	0.58±0.47	1.13±0.29	17.57±3.74	0.72±0.22	13.80±2.41	259.54±3.90	720.76±135.46
Winter	0.69±0.49	2.35±0.32	18.12±3.45	0.75±0.21	13.41±2.16	258.06±4.18	694.42±134.47
Spring	0.65±0.34	2.03±0.82	16.03±1.63	0.73±0.20	14.50±2.08	254.49±4.88	563.31±143.28
Summer	0.82±0.61	4.42±0.86	13.23±1.66	0.73±0.17	16.02±1.54	257.12±5.65	503.81±130.40
Autumn	0.60±0.42	2.53±1.06	14.78±3.32	0.65±0.21	14.71±2.12	262.93±4.40	677.80±138.64
Annual	0.69±0.48	2.83±1.44	15.54±3.21	0.72±0.05	14.65±1.03	258.15±3.58	609.84±109.60

Table 4. The detailed statistics obtained from the linear regression fitting for different aerosol and cloud parameters observed over the entire study domain from 2000-2017. The slope corresponds to the linear annual trend with the sign indicates negative or positive. Whereas the p-values with ≤0.05 and 0.05<p<0.1 represent data significant at 99% and 90% confidence levels indicated with bold and italic, respectively. The rest is the least significant.

Parameter	Unit	Mean (±SD)	Slope	Offset	p-value	Inter-annual variability	Percentage change in trend
AOD	Unit less	0.69±0.48	0.014	-26.269	0.003	0.695	**2.03**
WV	cm	2.83±1.44	-0.010	22.936	0.046	0.508	**-0.35**
COT	Unit less	15.54±3.21	-0.009	18.364	0.025	0.206	**-0.06**
CF	Unit less	0.72±0.05	0.003	-4.902	0.011	0.069	**0.42**
CER	micron	14.65±1.03	0.009	-3.626	0.483	0.070	0.06
CTT	K	258.15±3.58	-0.174	607.756	0.012	0.014	**-0.07**
CTP	hPa	609.84±109.6	-3.615	7868.794	0.002	0.180	**-0.59**

Table 5. Seasonal trends (year^{-1}) observed between AOD and cloud parameters during 2000−2017 over East China. The p-values with ≤0.05 and 0.05<p<0.1 represent data significant at 99% and 90% confidence levels indicated with bold and italic, respectively; whereas, the rest are least significant.

Parameter	DJF		MAM		JJA		SON	
	Trend	p-value	Trend	p-value	Trend	p-value	Trend	p-value
AOD	0.020	**0.003**	0.003	0.298	0.009	0.365	0.011	**0.027**
WV	-0.011	**0.003**	-0.020	**1.56e-4**	-0.036	**5.69e-4**	-0.017	*0.101*
COT	-0.049	0.691	0.038	0.428	0.004	0.852	0.021	0.833
CF	0.001	0.653	0.002	0.260	0.002	0.454	0.004	0.127
CER	0.052	**0.043**	-0.023	0.338	-0.040	**0.008**	-0.006	0.772
CTT	-0.073	0.323	-0.043	0.653	-0.005	0.937	-0.098	*0.925*
CTP	-1.234	0.381	-1.548	0.273	0.022	0.987	-2.772	*0.053*

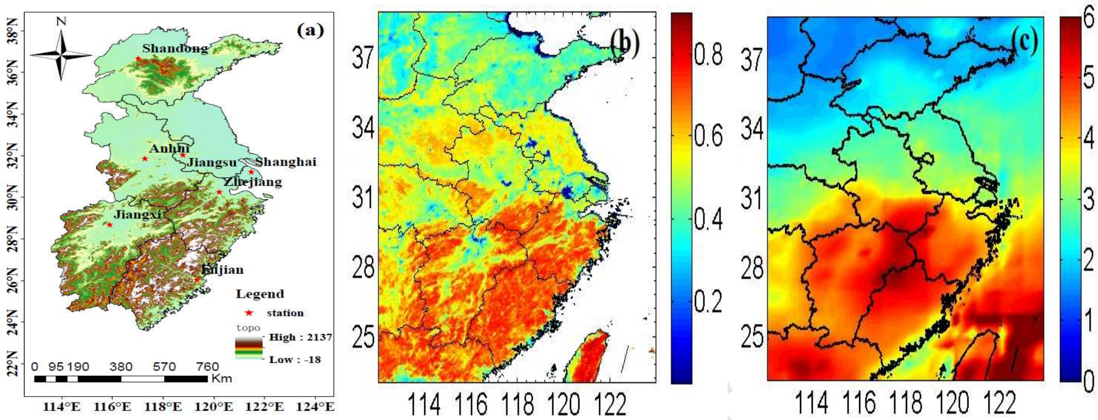

Fig. 1. (a) The terrain map representing elevation (in m) of East China using the DEM data. The province names were written inside the panel and the location of stations (see Table 1) considered in this study are pointed with a star symbol. Spatial changes of (b) NDVI and (c) precipitation rate (mm/h) retrieved from the MODIS and TRMM satellites, respectively observed over East China.

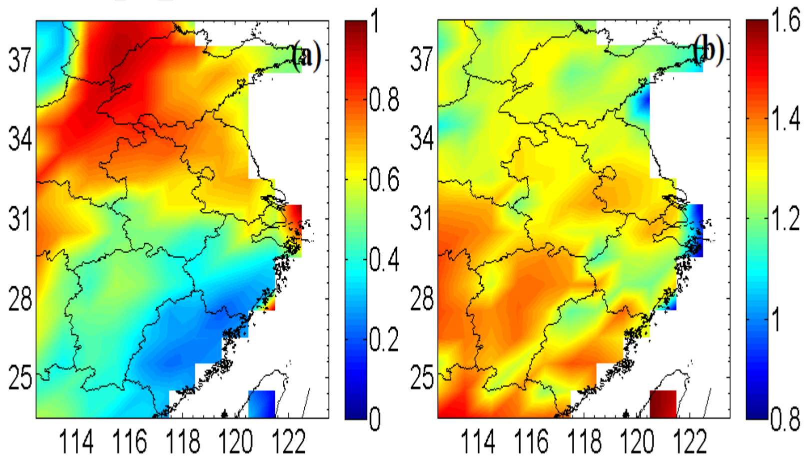

Fig. 2. The 18-year (2000-2017) averaged spatial variations of (a) AOD_{550} and (b) $AE_{470\text{-}660}$ observed over East China.

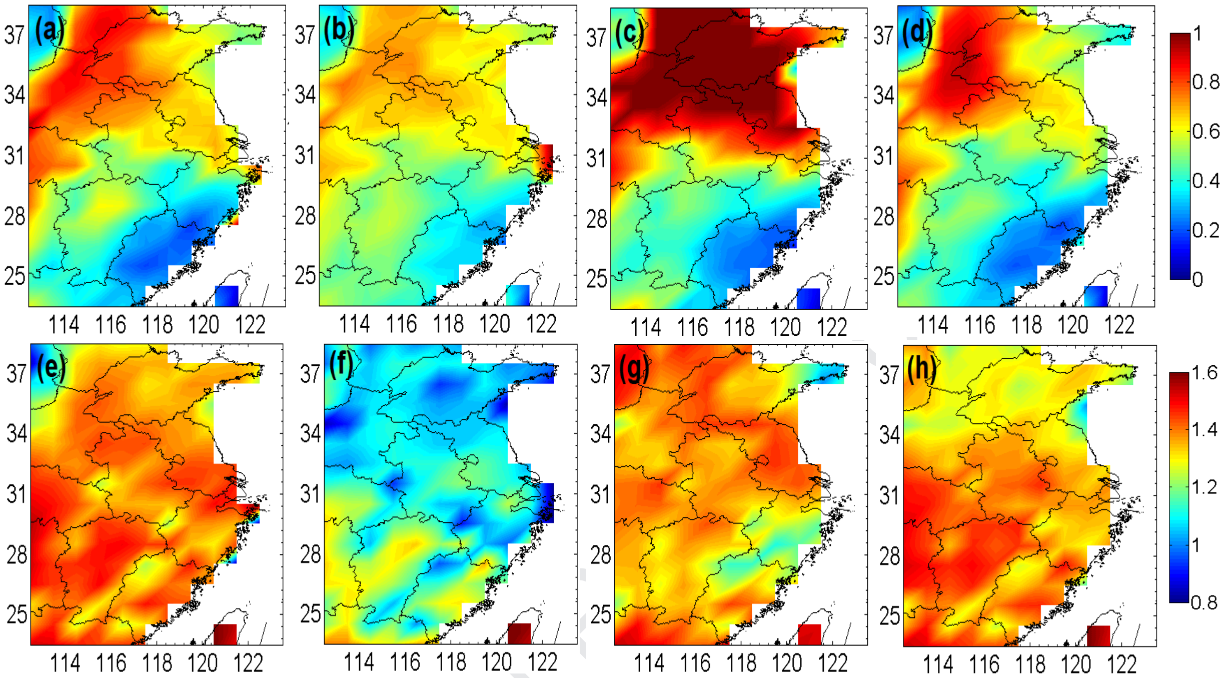

Fig. 3. Spatial distributions of seasonal mean changes in (a-d) AOD_{550} and (e-h) $AE_{470\text{-}660}$ retrieved from the MODIS for the study period over the study domain. The panels corresponds to different seasons with (a, e) winter (DJF), (b, f) spring (MAM), (c, g) summer (JJA), and (d, h) autumn (SON) seasons. The readers are advised to follow the similar seasonal sequence in the rest of figures.

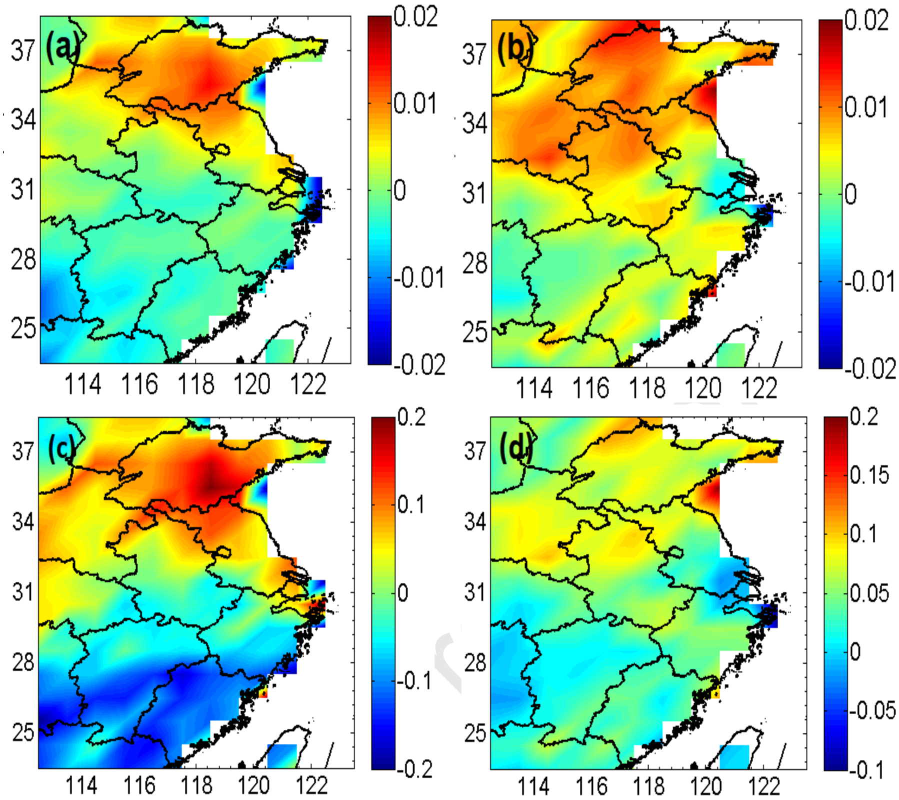

Fig. 4. Spatial maps of annual mean (top panels) tendencies and (bottom panels) relative tendencies in (a, c) AOD_{550} and (b, d) $AE_{470\text{-}660}$ over East China.

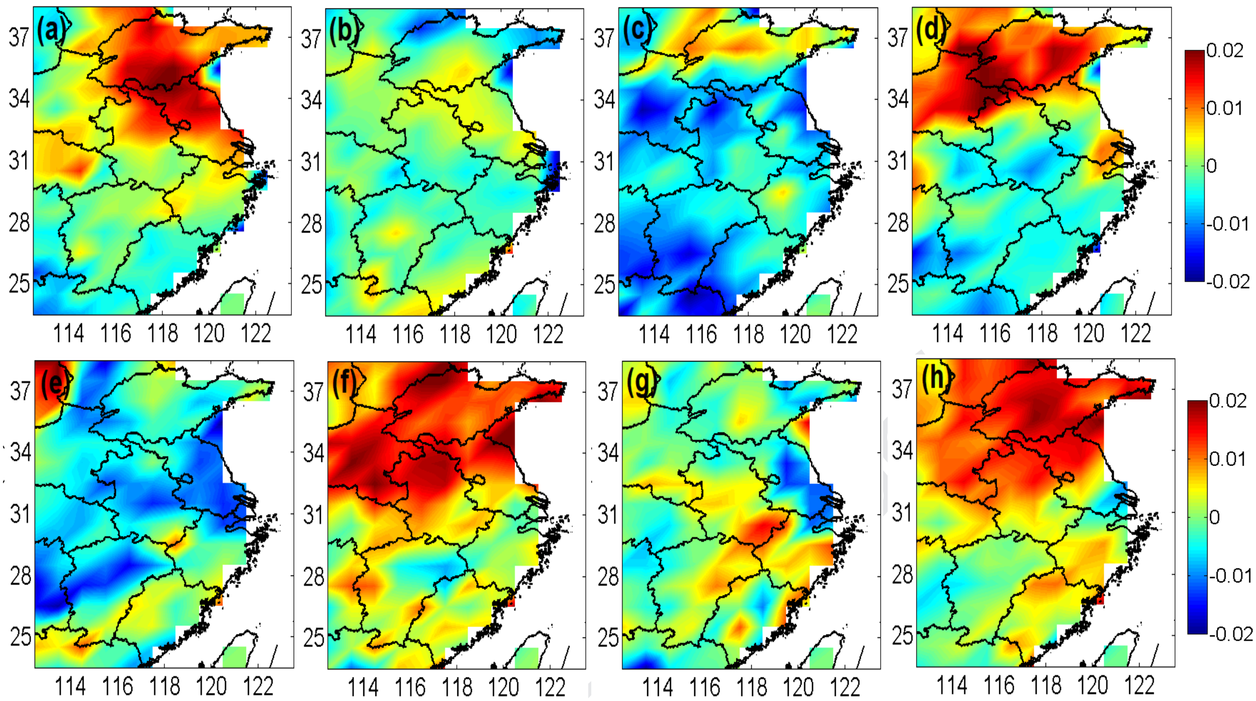

Fig. 5. Same as in Fig. 4, but for the seasonal mean tendencies in (a-d) AOD_{550} and (e-h) $AE_{470\text{-}660}$. The representation of seasons is same as mentioned in Fig. 3.

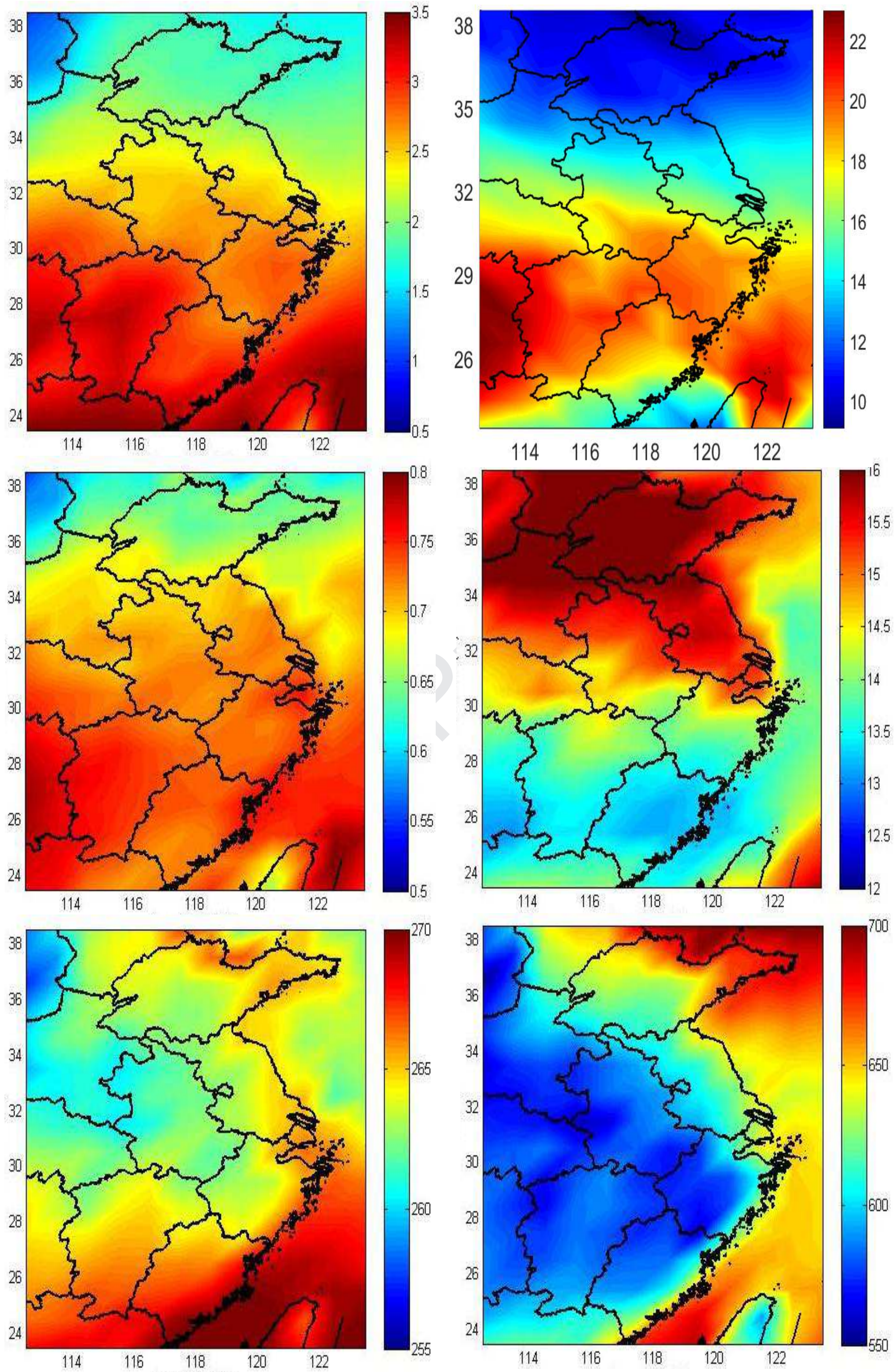

Fig. 6. Spatial variations of annual mean WV and cloud parameters retrieved from the MODIS Terra satellite during 2000-2017. The panels from left to right represent (top panels) WV (in cm) and COT (unit less), (middle panels) CF (unit less) and CER (in micron), and (bottom panels) CTT (in K) and CTP (in hPa).

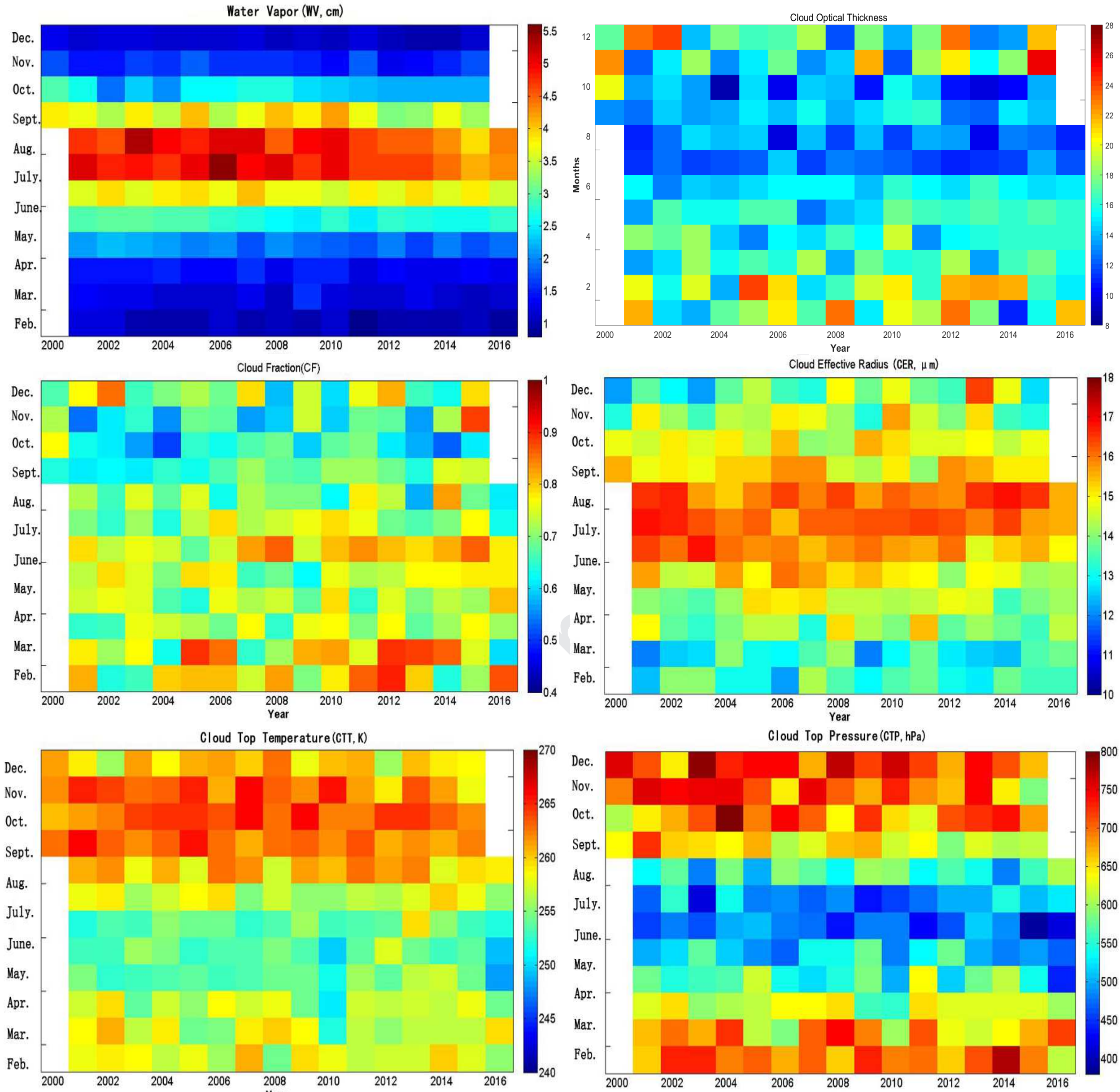

Fig. 7. Same as in Fig. 6, but on the temporal scale.

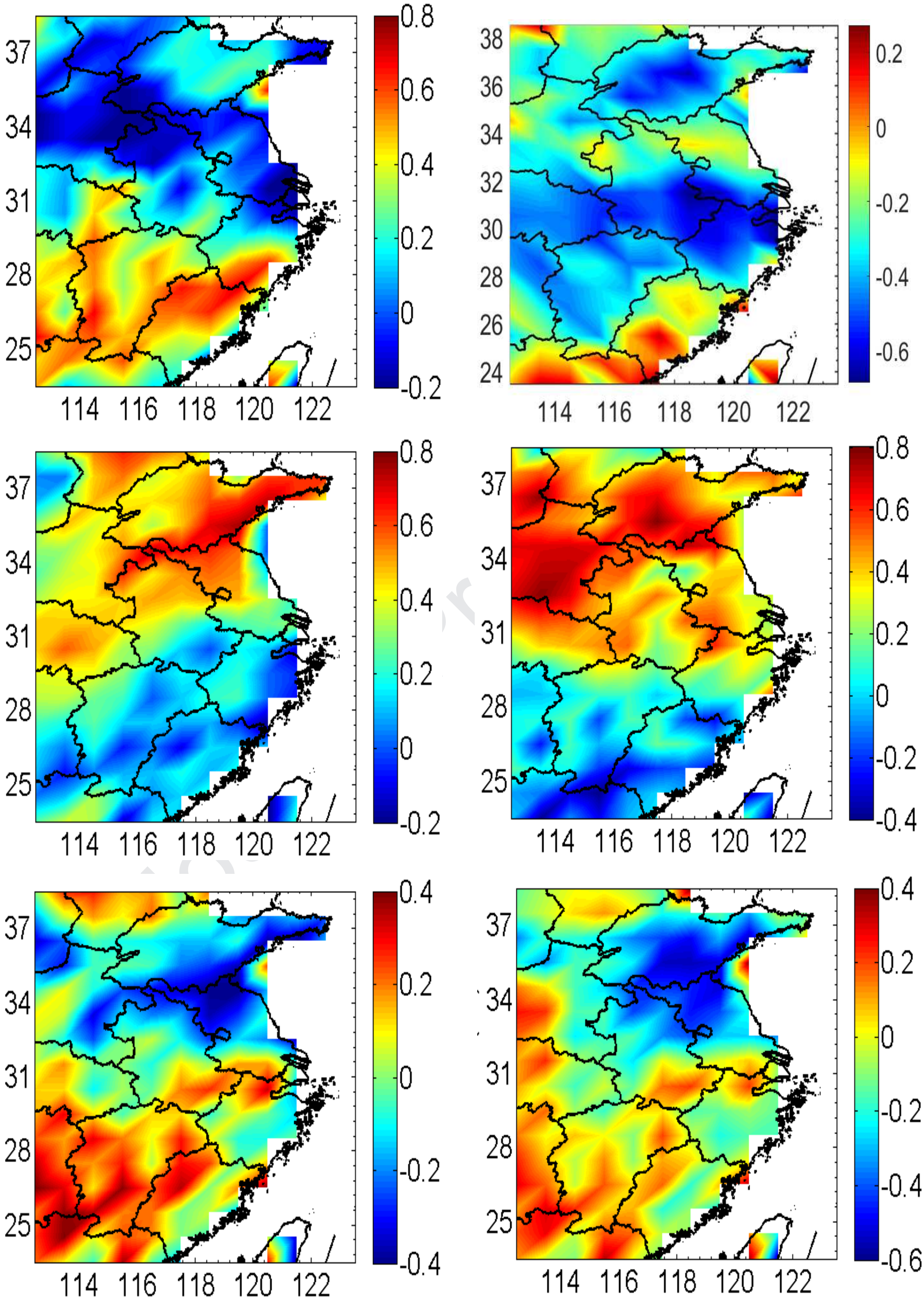

Fig. 8. Spatial correlations between (left to right panels) AOD and WV, and cloud parameters (such as COT, CF, CER, CTT, and CTP) observed from the MODIS.

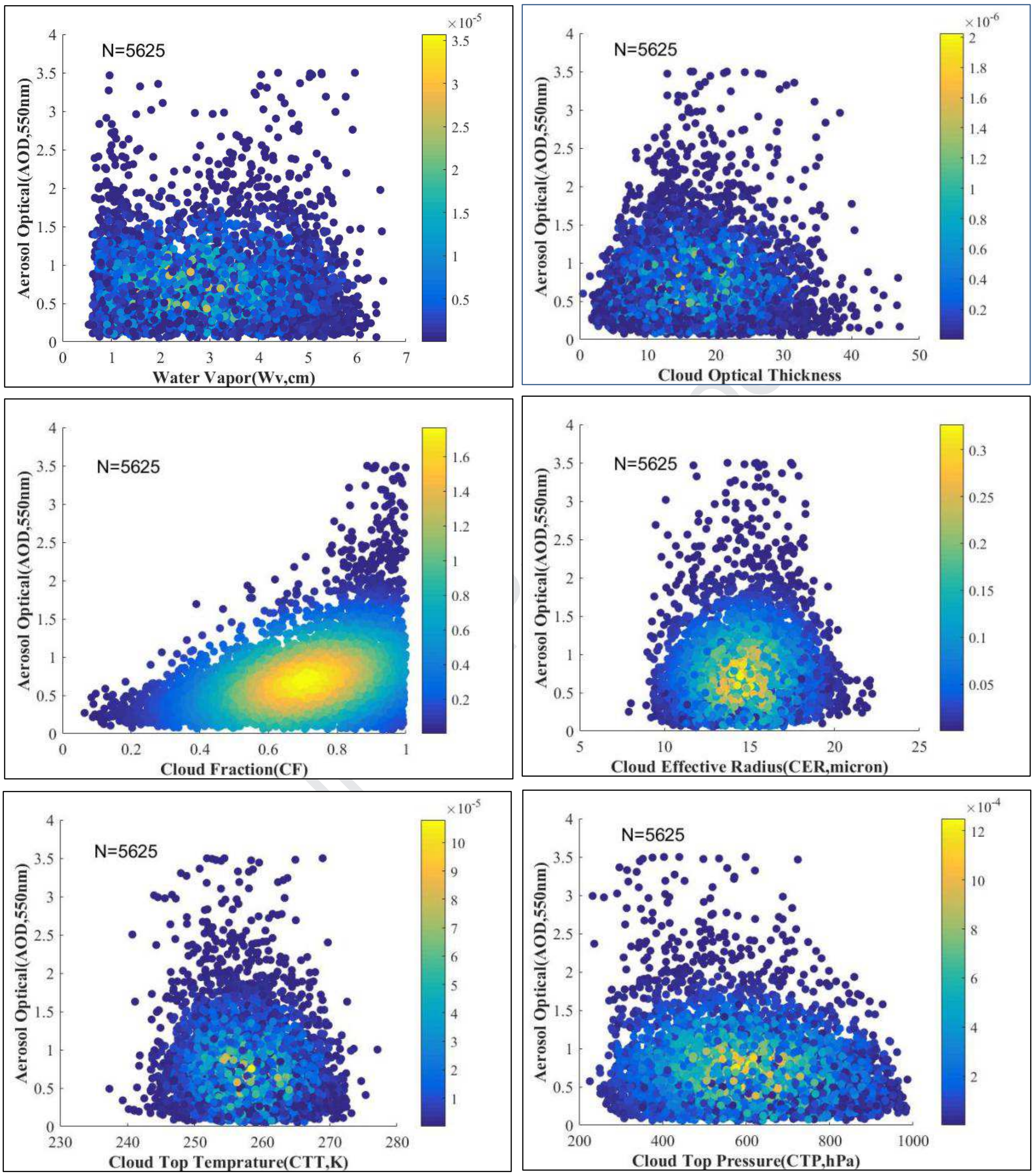

Fig. 9. Density scatter diagrams to examine the relationship between AOD_{550} and WV, and cloud parameters from all data points during the study period over East China. The number of samples used in the analysis is shown in all the panels. The corresponding statistics obtained from the regression analysis are given in Table S1 of SM.

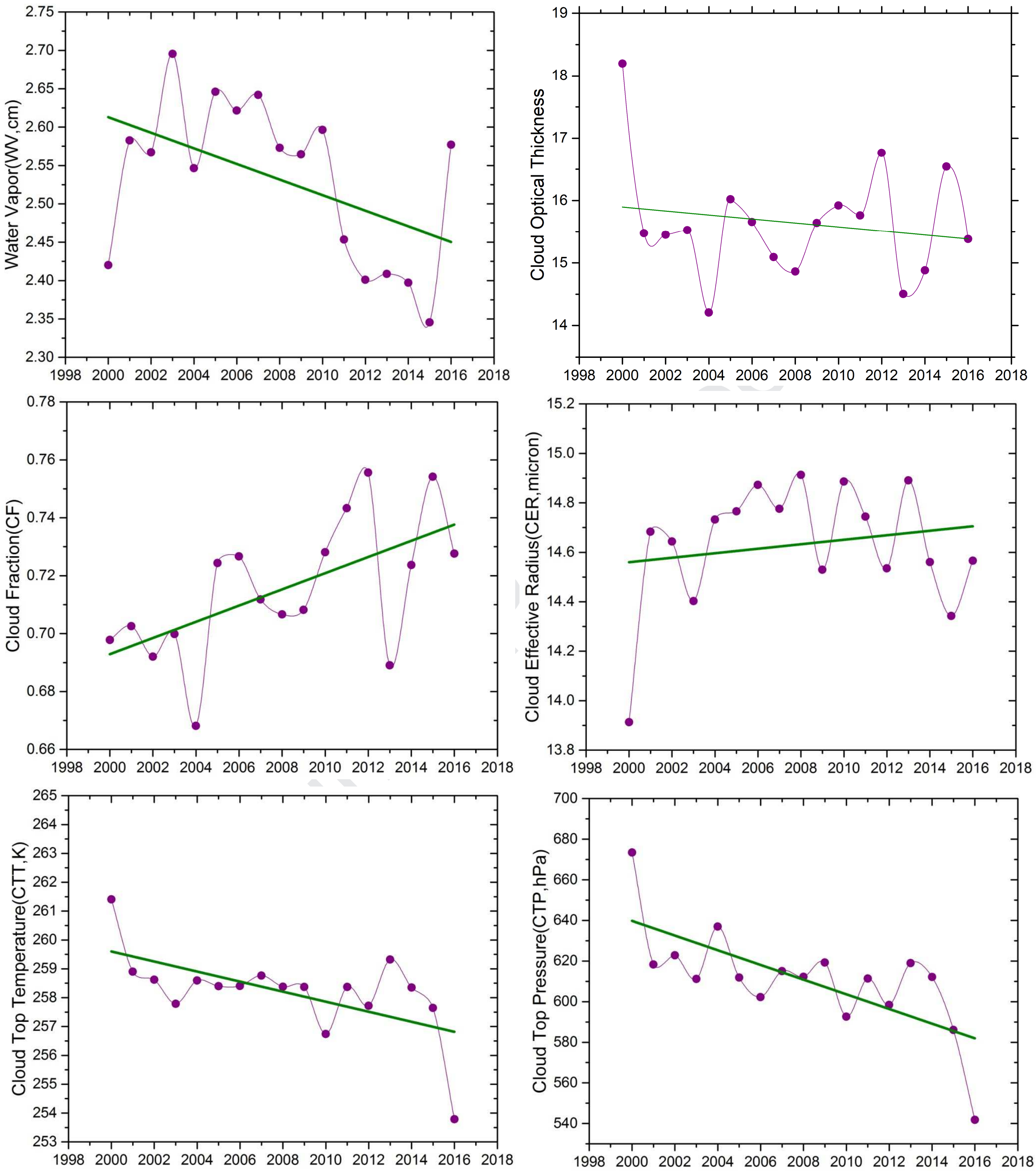

Fig. 10. Long-term linear trends in different aerosol and cloud optical properties over East China. The green solid line represents linear fitting to the data and the corresponding statistics obtained from the regression analysis are given in Table 4.

Research Highlights

- Aerosol and cloud properties exhibited substantial spatial and temporal variabilities in the recent years over East China.
- Significant increasing (decreasing) trend in AOD (CTT and CTP) was found over the Shandong Province in the North of the study domain.
- Moderate to high positive correlations were noticed between AOD and CER attributed to the dynamics played by the meteorology.

Statement of Declaration

The authors declare that they have no competing financial interests or personal relationships that could have appeared to influence the work reported in this paper.